

# Development of Nebivolol Hydrochloride Loaded Lipid Matrix -Nanoparticles-Gel for Treatment of Hypertension Via Transdermal Route: *Ex vivo* Permeation and *In vivo* Pharmacokinetic Study in Wistar Albino Rats

Parameshwar Kondapuram <sup>1</sup>, Srinivas Bhairy <sup>2</sup>, Shaik Harun Rasheed <sup>1</sup>,  
Subrahmanyam Pitchika <sup>3,\*</sup>

<sup>1</sup> Department of Pharmaceutics, School of Pharmacy, Gurunank Institutions Technical Campus (GNITC), Hyderabad, 501506, Telangana, India

<sup>2</sup> Department of Pharmaceutics, SSJ College of Pharmacy, Thane, 421 601, Maharashtra, India

<sup>3</sup> Department of Pharmaceutics, Vagdevi College of Pharmacy and Research Centre, Nellore 524 346, Andhra Pradesh, India

\* Correspondence: [subrahmanyam041@gmail.com](mailto:subrahmanyam041@gmail.com);

Received: 22.01.2025; Accepted: 11.04.2025; Published: 20.12.2025

**Abstract:** The study aimed to develop a nebivolol hydrochloride-loaded nanostructured lipid carrier-gel (NBH-NLC-gel) to enhance bioavailability when delivered transdermally. The NBH NLCs were produced via probe sonication followed by freeze-drying and were evaluated for their zeta potential, particle size, entrapment efficiency (EE), surface morphology, and drug loading. NLCs were tested for *in vitro* release, *ex vivo* permeability, and *in vivo* pharmacokinetics. The box-Behnken design was utilized to enhance the NBH NLC-gel for sustained transdermal delivery. The optimized batch was X<sub>1</sub> glyceryl monostearate = 179.45 mg, X<sub>2</sub> concentration of surfactant = 0.52% to achieve Y<sub>1</sub> (EE) = 89.11%, Y<sub>2</sub> (particle size) = 120 nm. The optimized NBH-NLC gel showed a 12 h release. *In vivo* pharmacokinetic studies showed a 3-fold improvement in bioavailability. The data suggest that NBH-NLC gels can be used for transdermal drug delivery to manage hypertension.

**Keywords:** nebivolol hydrochloride; nanostructured lipid carriers; pharmacokinetics; transdermal bioavailability.

© 2025 by the authors. This article is an open-access article distributed under the terms and conditions of the Creative Commons Attribution (CC BY) license (<https://creativecommons.org/licenses/by/4.0/>), which permits unrestricted use, distribution, and reproduction in any medium, provided the original work is properly cited. The authors retain copyright of their work, and no permission is required from the authors or the publisher to reuse or distribute this article, as long as proper attribution is given to the original source.

## 1. Introduction

Hypertension, or high blood pressure, is a medical disorder characterized by chronically elevated blood pressure, which can lead to cardiovascular disease [1]. Oral administration of anti-hypertensive medications has several drawbacks, including first-pass metabolism, limited intestinal bioavailability, and the lack of regulatory control over absorption rates [2-4]. NLCs are relatively novel lipid nanoparticles with promising potential as a medication delivery vehicle. NLCs offer a diverse delivery strategy, with the potential for transdermal medication administration. NLC has relatively low cytotoxicity. They have a solid matrix for regulated medication release, rather than the burst release observed with emulsions [5,6]. Due to their small size, lipid particles may make direct contact with the stratum corneum, increasing the skin's ability to absorb drugs. This carrier's solid lipid matrix makes it possible to achieve

regulated release [7]. In cases when prolonged dosing and increased systemic absorption are required [8], this becomes a vital strategy [9]. In recent years, NLC has emerged as an established new drug delivery system, especially for dermal and transdermal applications. Nebivolol hydrochloride (NBH) is a biopharmaceutical categorization system (BCS) class II molecule with log P 3.21 [10].

Additionally, the oral administration of NBH is frequently restricted in treating hypertension due to concerns such as overactive hepatic function, inter-subject variability, and gastrointestinal problems. Due to its low molecular weight (441.9 Da), high log P (3.21), and low therapeutic dosages (5-10 mg), it takes around 1.5–4 h to achieve an effective plasma concentration [11]. The transdermal route has several advantages over the oral route, such as minimizing dose frequency, preventing hepatic first-pass metabolism, lessening gastrointestinal side effects, and increasing patient compliance [12]. NBH skin penetration profile via the transdermal route has been described in the past. However, a notable plasma concentration was not attained [13]. The present study evaluated the viability of NLCs as a novel transporter system for the transdermal delivery of NBH, focusing on the regulation of NBH skin permeability with Capryol 90 and glycerol monostearate, a solid lipid. After establishing and modifying formulations using a three-factor, two-level Box-Behnken design, the particle size, shape, effective entrapment, *ex vivo* skin penetration, morphology, *in vitro* release, and pharmacokinetics were assessed.

## 2. Materials and Methods

### 2.1. Materials.

NBH was acquired as a gift sample from MSN Laboratories Pvt Ltd (Hyderabad, India), and Capryol 90 was obtained from Gattefosse India Pvt. Ltd. (Mumbai, India). Both Glycerol monostearate and Tween 80 were obtained from SD Fine Chemicals Limited (Mumbai, India). Hi-media Laboratories Pvt. Ltd. (Mumbai, India) was the supplier of the dialysis membrane. Triethanolamine and Carbopol 940 were acquired from RFCL Laboratories Pvt. Ltd (Hyderabad, India). All other analytical grade chemicals and solvents were procured from SD Fine Chem (India).

### 2.2. Screening of lipids.

A semi-quantitative method was used to determine the solubility of NBH in solid lipids. Briefly, solid lipids such as glycerol monostearate, tartaric acid, myristic acid, precious ATO 5, and tripalmitin were melted individually above their melting points (5-10°C) in a controlled water bath. The NBH was added and checked for complete solubilization of NBH [14,15]. For liquid lipids, NBH was added to oleic acid, isopropyl myristate, capryol 90, coconut oil, and sunflower oil individually in screw-top glass tubes, which were placed in a shaker incubator (Oscar Equipment, India) for 48 h at room temperature. The specimen vials were spun for 10 min (REMI centrifuge, India), and the supernatant was collected for a UV-visible spectrophotometer (Shimadzu 1800, Japan) at 282 nm. Triplicate tests were performed [16].

### 2.3. Preparation of NBH NLC.

Box-Behnken was used to create several NLC formulations, and Design-Expert® software (Trial version 13.0.1.0; Stat-Ease Inc., USA) was used to construct experimental runs [17,18]. In brief, the EE (Y1) and particle size (Y2) were selected as independent variables, and the NLCs containing NBH were developed through a previously published probe sonication (Oscar Ultrasonics Pvt Ltd., India) and freeze-drying process [19]. To dissolve Tween 80, we heated 50 mL of the aqueous phase to 60°C, while glycerol monostearate, Capryol 90, and NBH were diluted to a 10 mL solution in dichloromethane. The oily segment was inserted into the liquid one drop at a time in 50 mL tubes, and the mixture was centrifuged (Remi Pvt Ltd., India) for 20 min at 8000 rpm. Centrifuged samples and supernatant were evaluated for EE [20].

### 2.4. Optimization of NLC using Box-Behnken design.

A 2-factor, 2-level Box-Behnken study was conducted to assess the interactions among surfactant, lipid, and the liquid lipid/total lipid ratio in the formulations. Below is a nonlinear computer-generated quadratic model for the 17 experimental runs produced by trial version design expert® software (version 13.0.1.0; State-Ease, 16 Inc., Minneapolis, USA).

Each combination of component levels elicited a unique response, which was accounted for by the intercept ( $b_0$ ), the linear coefficients ( $b_1$ ,  $b_2$ , and  $b_3$ ), the interaction coefficients ( $b_{12}$ ,  $b_{23}$ , and  $b_{13}$ ), and the quadratic coefficients ( $b_{11}$ ,  $b_{22}$ , and  $b_{33}$ ). A surfactant (Tween 80) was used as an independent variable ( $X_1$ ). Particle size ( $Y_1$ ) and EE ( $Y_2$ ) were the dependent variables; total lipid (glyceryl monostearate + capryol 90) was the independent variable (equation 1). We settled on our final independent variables based on the outcomes of many pilot studies. A range of surfactant concentrations (-1, 0, +1), total lipid concentrations (-1, 0,+1), and liquid lipid to total lipid ratios were examined. As shown in Table 1, several formulations were developed based on the selected independent variables.

$$Response = b_0 + b_1X_1 + b_2X_2 + b_3X_3 + b_{12}X_1X_2 + b_{13}X_1X_3 + b_{23}X_2X_3 + b_{11}X_1^2 + b_{22}X_2^2 + b_{33}X_3^2 \quad (1)$$

**Table 1.** Box-Behnken design's dependent and independent variables are utilized to develop and optimize NBH NLC.

Variables	Levels		
	Low (-1)	Medium (0)	High (+1)
Independent Variables (factors)			
$X_1$ = Surfactant	100	150	200
$X_2$ = Concentration of Total lipid (% w/v)	0.50	0.75	1
Dependent variables (response)			
$Y_1$ = EE (%)	Maximize		
$Y_2$ = Particle size (nm)	Minimize		

### 2.5. Particle size analysis.

The average particle size of the NLC was determined by dynamic light scattering (DLS) at  $25 \pm 1^\circ\text{C}$ ,  $90^\circ$  scattering angle, using a computerized inspection system and a Malvern nano-zeta-sizer (Malvern Instruments, Nano Z.S., U.K.), and analyzed using 'DTS nano' software. Freeze-dried NLC (1 mg) was reconstituted in double-distilled water (0.5 mL). Three measurements of each size were collected [21,22].

## 2.6. Zeta potential measurement.

Zeta potential was measured using the technique of laser Doppler micro-electrophoresis by Malvern Zeta Sizer ZS90 (Malvern Instruments, Nano Z.S., U.K).

## 2.7. Entrapment efficiency (EE) and drug loading (DL).

The effectiveness of entrapment was evaluated by using an ultracentrifuge for filtration, equipped with an ultrafilter, as previously described [23]. Tenfold dilutions of NLC dispersion were placed in a centrifuge tube and centrifuged for 45 min at 4000 rpm (Remi centrifuge, India) (equation 2). To evaluate drug loading, freeze-dried NLC was dissolved in an ethanol/chloroform mixture (50:50) and filtered through a 0.45  $\mu$  membrane filter. The filtrates, at suitable dilutions, were analyzed using a UV-visible spectrophotometer (Shimadzu 1800, Japan) [24] (equation 3).

$$EE(\%) = \frac{\text{Total amount of drug} - \text{unentrapped drug}}{\text{total drug}} \times 100 \quad (2)$$

$$DL(\%) = \frac{\text{Amount of drug into NLC}}{\text{Total weight of NLC}} \times 100 \quad (3)$$

## 2.8. Scanning electron microscopy (SEM).

SEM (Hitachi, S-3700N, Tokyo, Japan) helps to understand the surface morphology of NLCs. Freeze-dried NLCs were reconstituted in double-distilled water, then sprinkled onto silicon, and allowed to dry at room temperature overnight before being affixed to the metal stub using double-sided adhesive tape for analysis. The samples were sputtered and coated with gold in a vacuum using a 20 kV scanning electron microscope [25].

## 2.9. Differential scanning calorimetric (DSC) analysis.

DSC (Shimadzu DSC-60, Tokyo, Japan) was performed using 3 mg of each sample, which were packed in a standard aluminum temperature range of 30°C-400°C, with nitrogen purging at 20 mL/min to allow a scanning rate of 5°C/min.

## 2.10. Preparation of NLC gel.

For the development of the gel system, Carbopol 934 at 0.61-1.2% (w/w) was dissolved in water, mixed, and then allowed to hydrate in the dark. Both the NBH conventional gel and the NBH NLC gel contained polyethylene glycol (PEG)-400 (15.0% w/v) as a plasticizer and 1,8-cineole as a skin permeation enhancer [26,27]. Triethanolamine (0.5% w/v) was used to neutralize the gel dispersion. After adding half of the remaining water to the preformed gel base, NBH NLC dispersion was added while stirring slowly. The viscosity of the produced gel was measured by a Brookfield digital viscometer (Model DV-II, USA) equipped with a spindle S27. The spreadability of the NBH NLC gel was evaluated by stroking (0.5 g) of gel within 1 cm-diameter sphere on a glass plate and then placing a second glass plate on top. It was performed at room temperature following a 3-minute pause. 5 min were spent with a 500 g weight resting on the glass plate. As the gels spread, pre-marked gel regions swelled in size [28].

### 2.11. *In vitro* release study.

The release study was performed using the dialysis bag method. The volume of the receptor compartment (reservoir) in the experimental cell was 5 mL, and the diffusion area of the cell was 4.52 cm<sup>2</sup>. The NBH NLCs and the plain NBH were separately dissolved in phosphate buffer, pH 7.4, and placed in a donor compartment. In the receiver chamber, a solution of ethanolic phosphate buffer (30:70) was maintained at 37°C with stirring at 100 rpm. Consistent conditions were maintained by frequently switching vehicles to transport 1 mL of samples from the sink. The concentrations of NBH were determined using a UV-visible spectrophotometer (Shimadzu 1800, Japan) at a wavelength of 282 nm [29].

### 2.12. *Ex vivo* skin permeation study.

Franz's diffusion cells (LabIndia Analytical, India) were used to examine *in vitro* the penetration of rat skin. Phosphate-buffered saline was used to remove the surgically removed fat from the rat's skin. After preparation, the stratum corneum-facing dermis shall be placed between the donor and receiver compartments of the Franz diffusion cell (surface area: 0.78 cm<sup>2</sup>; receiver measurements fraction: 5 mL), with the "donor compartment" on the outside. The Franz diffusion cell was placed on a magnetic stirrer rotating at 100 rpm, with the temperature maintained at 37°C. The donor compartment contains NBH NLC gel equivalent to 1 mg of NBH. At 1, 2, 4, 6, 8, 10, and 24 h, the ethanolic phosphate buffer (30:70) in the receiver compartment was replaced with an equal volume of ethanol in phosphate buffer. The same process was repeated for conventional NBH gel. The concentrations of NBH were determined using a UV-visible spectrophotometer (Shimadzu 1800, Japan) at a wavelength of 282 nm [30,31].

### 2.13. *In vivo* pharmacokinetic study.

The Guru Nanak Animal Ethics Committee examined and approved the animal protocol for this pharmacokinetics investigation (Protocol No. GNIP/CPCSEA/IAEC/2019/07). *In vivo* tests were conducted on Wistar albino rats of reproductive age (210 - 300 g). The rats were separated into "three groups" (n = 6) after their backs were clean-shaven. Group 1 was administered an oral tablet (as suspension) of NBH (Nebimax 1 Tablet, Smith and Kenner Pharmaceuticals Pvt. Ltd). In contrast, Groups 2 and 3 were given topical formulations of NBH conventional and NBH NLC gel with 1,8-cineole, respectively. Blood was collected into disodium ethylenediaminetetraacetic acid stored in Eppendorf tubes at 0, 0.5, 1, 2, 3, 4, 6, 8, 12, and 24 h. We separated the plasma by centrifuging the samples (REMI centrifuge, India) for 15 min at 5000 rpm and analyzed them by high-performance liquid chromatography [32]. Plasma concentration-time profiles were generated, with average and standard deviation values, and an intensity plot was constructed for each time point. Plasma concentrations were computed, and graphs were constructed with the Y-axis showing concentration and the X-axis showing time. Using the concentration data acquired using the Kinetic 2000 software. The AUC<sub>(0-t)</sub> and pharmacokinetic parameters (C<sub>max</sub>, T<sub>max</sub>) of each formulation were determined.

#### 2.13.1. Statistical analysis.

*Ex vivo* and *in vivo* pharmacokinetic research findings were compared using analysis of variance (ANOVA) and T-Tests, and statistically significant differences were resolved at the 95% confidence level (p ≥ 0.05). Graph-Pad Software Inc.'s trial version of Graph Pad <https://nanobioletters.com/>

I.N.S.T.A.T. was utilized for evaluation (San Diego, USA). The mean and standard deviation were calculated for the entire data set. Dunnett's test and one-way ANOVA on data were conducted by GraphPad Prism 5, USA software, in which  $p < 0.05$  indicates a considerable difference.

### 3. Results and Discussion

#### 3.1. Screening of lipids.

The ability of NLC to retain the drug is directly proportional to the drug's solubility in the lipid matrix [33]. In the creation of NLC formulations, the solubility of poorly soluble drugs in oils is one of the most crucial factors in selecting liquid lipids. The oil content of NLC profoundly affects particle size, surface shape, EE, and drug release. NBH showed the highest solubility in Capryol 90 ( $8.10 \pm 0.25$  mg/mL), which was selected as the oil phase for NLC production. NBH exhibited the highest solubility in glyceryl monostearate ( $93.44 \pm 0.50$  mg/mL) and was selected as the solid lipid core. Additionally, it has been claimed that glyceryl monostearate is compatible with Capryol 90 [34].

#### 3.2. Optimization of NLC by Box-Behnken design.

Several methods of hit-and-trial experiments were used to determine which independent factor was most important. In the end, surfactant and total lipid were shown to impact NLC's ultimate form. Table 2 summarizes the replies to Box-Behnken's 17 distinct formulations.

**Table 2.** The response shown in the Box-Behnken design for optimizing NBH NLCs is compared to the expected values from the design expert software.

Runs	Independent variables		Dependent variable			
	X <sub>1</sub>	X <sub>2</sub>	Y <sub>1</sub>		Y <sub>2</sub>	
			Actual value	Predicted value	Actual value	Predicted value
1	0	-1	85	84.4	125	121
2	+1	-1	86	84.4	120	121
3	0	+1	87	88	113	129.125
4	+1	+1	89	88	100	97.25
5	+1	0	91	90	82	97.875
6	0	+1	94	94	72	67.625
7	0	0	84	84.4	124	121
8	0	0	85	87	110	97.25
9	0	-1	86	87	112	108.25
10	0	0	88	86	90	108.25
11	0	0	90	89	81	91.625
12	-1	+1	93	93	83	87.875
13	0	0	83	84.4	125	121
14	+1	0	84	84.4	110	121
15	-1	0	85	86	144	133.875
16	-1	0	87	89	120	97.875
17	-1	-1	89	87	140	129.125

Figure 1 shows three-dimensional graphs of the Y1 and Y2 responses. These plots help examine the combined effects of two variables on response, the effects of a single variable, and the interaction between that variable and another. The reaction values obtained in the experiments were quantitatively compared with the expected values (Figure 2).

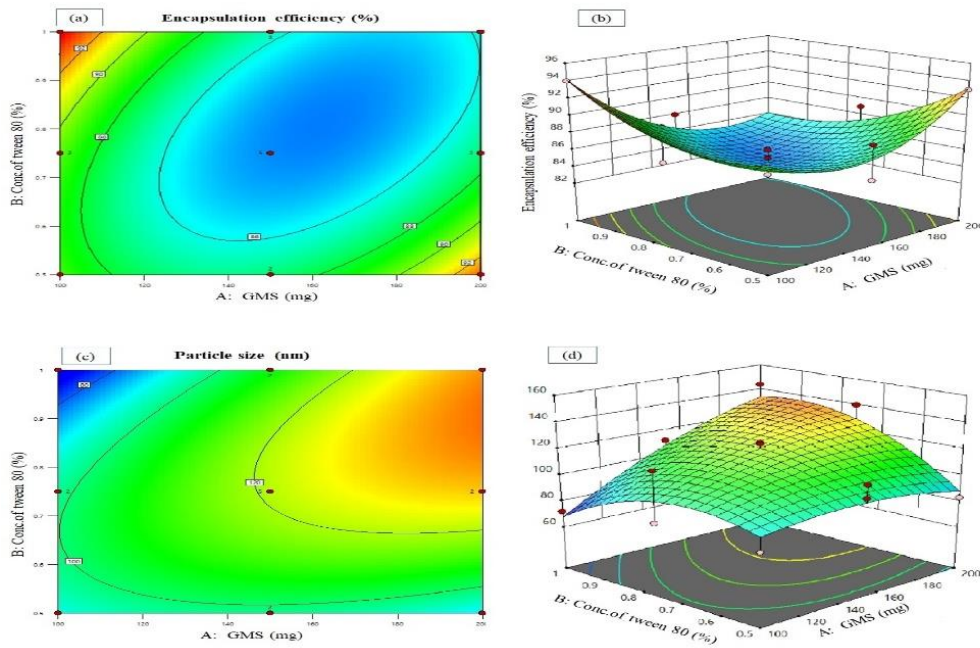


**Figure 1.** Response surface plots showing the simultaneous influence of independent variables on response parameters EE and vesicle size within Box–Behnken experimental design.

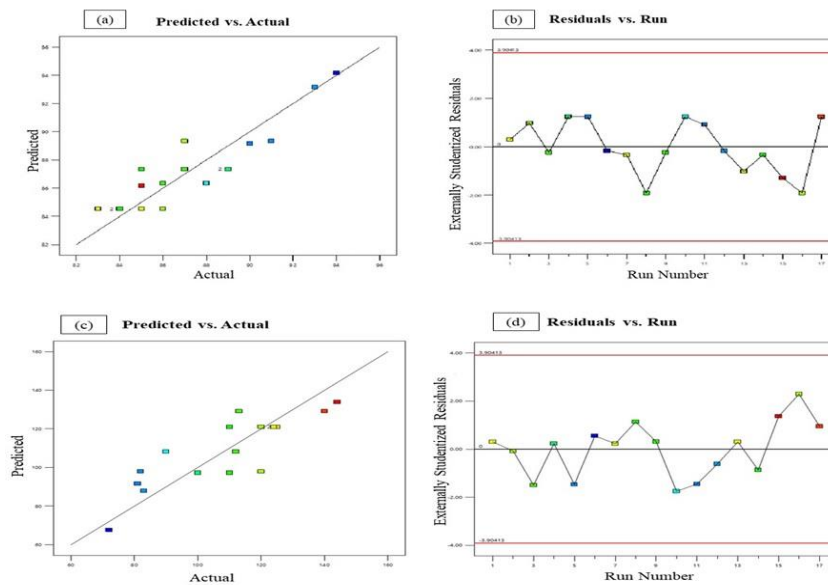


**Figure 2.** (a) Linear correlation plot between actual and predicted values for response EE; (b) residual plot for response EE; (c) Linear correlation plot between actual and predicted values for response vesicle size; (d) residual plot for response vesicle size.

Based on 17 data experiments, the nonlinear program identified a quadratic model with a correlation coefficient of approximately 1 as the best fit for all three dependent variables. 0.8198 for the entrapment efficiency  $R^2$  indicates a strong match, whereas 0.5429 for the anticipated  $R^2$  is in fair agreement with 0.7378 for the adjusted  $R^2$ . The particle size  $R^2$  correlation was calculated and found to be 0.7138, indicating a close match. There is a decent match between the two sets of data, with the projected  $R^2$  of 0.1308 being in fair agreement with the corrected  $R^2$  of 0.5837 (Table 3).

**Table 3.** A summary model was fitted to the observed data.

	R <sup>1</sup>			R <sup>2</sup>		
	F Value	P Value	Remarks	F Value	P Value	Remarks
Linear	6.82	0.0081		2.99	0.0774	
2FI	5.90	0.0141		2.32	0.1395	
Quadratic	0.4634	0.7157	Suggested	0.8946	0.4847	Suggested
Cubic	0.1203	0.7377	Aliased	0.0049	0.9457	Aliased

It has been determined that the dependent variables NLC EE and particle density have values between 83± 2.50% and 94± 4.60% and 72± 2.81 nm and 140± 2.60 nm, respectively. Each term in a polynomial equation may be either positive or negative, with positive values indicating a positive association between the independent variable and the final solution and negative values indicating the reverse relationship. Effects of surfactant concentration (X<sub>1</sub>) on EE and particle size are distinct from those of surfactant concentration (X<sub>2</sub>). Less so than particle diameter, total lipid (X<sub>2</sub>) was shown to benefit EE (Table 4).

**Table 4.** Model response summary statistics to pick a data-fitting model.

	R <sup>1</sup>				R <sup>2</sup>			
	R <sup>2</sup>	Adj. R <sup>2</sup>	Pre. R <sup>2</sup>	PRESS	R <sup>2</sup>	Adj. R <sup>2</sup>	Pre. R <sup>2</sup>	PRESS
Linear	0.0609	-0.0732	-0.5698	257.62	0.3052	0.2060	-0.1834	8510.37
2FI	0.2803	0.1142	-0.8554	304.50	0.4756	0.3545	-0.2624	9078.77
Quadratic	0.8198	0.7378	0.5429	75.02	0.7138	0.5837	0.1308	6250.79
Cubic	0.8441	0.7229	0.4298	93.59	0.7856	0.6188	0.3610	4595.41

Comparing the effect of concentration on particle size to its effect on EE a reduction of approximately 330% was observed. The proportion of liquid lipids to total lipids will have a 130% greater effect on particle size than EE. In addition, the outcomes demonstrated that particle size was more sensitive to variations in surfactant concentration (X<sub>1</sub>) and lipid concentration with the oil-to-total lipid ratio (X<sub>2</sub>) than to drug loading or EE (equations 4 and 5) (Table 5).

**Table 5.** Analysis of variance chart for observed data.

Source	R <sup>1</sup>		R <sup>2</sup>	
	F Value	P Value	F Value	P Value
Model	10.01	0.0008 <sup>a</sup>	5.49	0.0089
A-Concentration of Glyceryl monostearate	2.98	0.1125	10.44	0.0080
B-Concentration of Tween 80	0.7438	0.4069	1.29	0.2796
AB	13.39	0.0038 <sup>a</sup>	6.55	0.0266 <sup>a</sup>
A <sup>2</sup>	22.86	0.0006 <sup>a</sup>	1.27	0.2839
B <sup>2</sup>	8.42	0.0144	7.52	0.0192 <sup>a</sup>
Lack of Fit	0.4634	0.7157	0.8946	0.4847
S.D	1.64		13.68	
C.V%	1.88		12.56	
Adj. R <sup>2</sup>	0.7378		0.5837	
Pre. R <sup>2</sup>	0.5429		0.1308	
Adeq. Precision	9.8867		8.1521	

<sup>a</sup> 0.0001 < p < 0.05.

$$EE = 84.53 - 1.0000A - 0.5000B - 3.00AB + 3.82A^2 + 2.32B^2 \quad (4)$$

$$Particle\ size = 121 + 15.63A + 5.50B + 17.50A - 7.50A^2 - 18.25B^2 \quad (5)$$

Optimized NBH NLCs were selected to maximize EE and minimize particle size using the Design-Expert point-prediction optimization approach. The formulation composition, including surfactant (150 mg) and total lipid (0.75%), met the requirements for improved NBH NLCs. These experimentally observed values of EE (84.48%) and particle size (120.12 ± 2.10 nm) presented by the optimized NBH NLCs agreed with the predicted values of particle size

(121.41 nm) and EE (84.44 %) generated by design expert software, indicating that the optimized formulation was reliable and rational (Figure 1).

### 3.3. Particle size analysis.

The analysis indicates that sonication of the NLC dispersion may effectively decrease particle size and narrow the particle size distribution. With a PDI of  $0.217 \pm 0.041$  and an average particle size of  $120.687 \pm 2.13$  nm, the optimized NBH NLCs scattering was discovered to have a narrow particle size distribution (Figure 3a). The observed particle size was  $150.1 \pm 2.60$  nm, and the PDI was determined to be  $0.239 \pm 0.055$  after lyophilization. It was found that surfactant quantity had a greater effect on particle size than overall lipid content. A shift in particle size caused by a change in the ratio of liquid to solid lipids may be attributed to a change in viscosity. Indicates that the system's composition substantially impacts the average particle size of the NLC dispersion.

### 3.4. Zeta potential measurement.

The zeta potential for optimized NBH NLC was found to be  $-30.40 \pm 0.12$  mV, whereas it was  $-31.51 \pm 0.14$  mV after lyophilization. The stability of aqueous dispersion over the long term is indicated by a zeta-potential value greater than 30 mV. (Figure 3b).

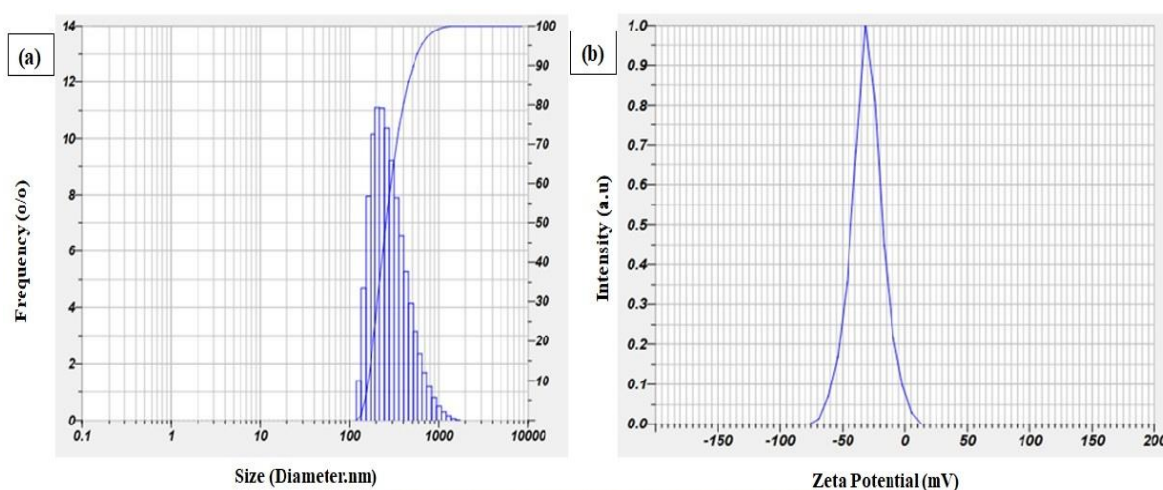


**Figure 3.** (a) particle size distribution; (b) zeta potential optimized NBH NLC.

### 3.5. Entrapment efficiency and drug loading.

EE of  $84.45 \pm 2.60$  % was determined for NBH NLC after optimization. Drug solubility in solid lipids and liquid lipids, as well as drug partitioning among the oil and aqueous phases, are primarily responsible for the entrapment. The drug loading of the prepared, optimized NBH NLC was determined to be  $12.55 \pm 2.27$  %. This high drug loading was due to NBH's higher solubility in the solid lipid (glyceryl monostearate). In contrast, comparably low drug loading is observed in the lyophilized NLC, possibly due to the loss of some carriers during lyophilization.

### 3.6. Scanning electron microscopy.

SEM of the optimized NBH NLC is shown in Figure 3c. It revealed the formation of well-identified spherical, discrete particles and displayed the retention of solid particulate structure.

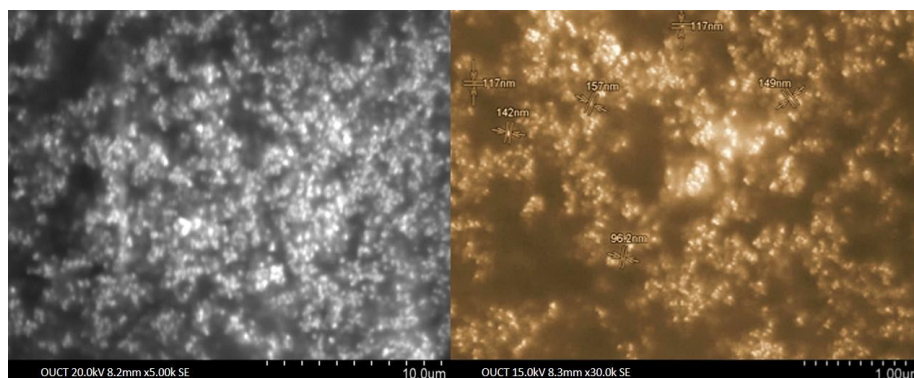


**Figure 4.** Scanning electron micrograph of the optimized NBH NLC.

### 3.7. Differential scanning calorimetric (DSC) analysis.

NBH, placebo NBH, NBH NLC physical mixture, glyceryl monostearate, and NBH NLC displayed an endothermic peak at 233.3°C, 124.4°C, 110.4°C, 58.5°C, and 201.4°C, respectively, on the individual DSC thermogram (Figure 5). Due to NBH solubilization in molten glyceryl monostearate before its melting point is reached, the melting endotherm of NBH in the physical combination disappears. In a similar vein, the melting endotherm of NBH disappearing into NLC can be explained by the drug being solubilized, molecularly dispersed, or converted into an amorphous form, while the movement and splitting of the glyceryl monostearate endothermic peak in the placebo NLC and NBH NLC thermograms can be related to the drug changing the glyceryl (solid lipid). The above property may underlie the substantial amount of drug packed into the NLC matrix.

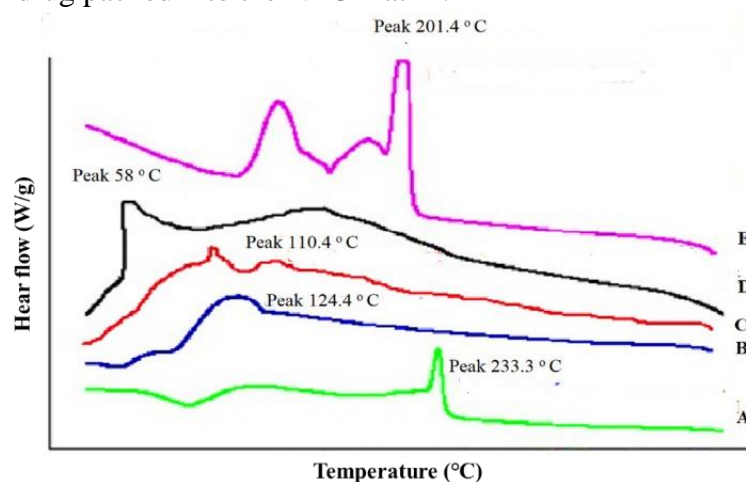


**Figure 5.** DSC thermogram of: (A) NBH; (B) Placebo NLC; (C) NBH NLC physical mixture; (D) Glyceryl monostearate; (E) NBH NLC

### 3.8. Preparation of gel.

The NLC was subsequently made into a gel for easy delivery to the skin of experimental rats. Carbopol 934 was employed to make gel compositions at concentrations of 0.6, 0.75, and 1.0 % w/w. The gels' viscosity and spreadability were used to determine that 1% w/w Carbopol 934 was the optimal concentration. NBH NLC gel was clear, devoid of particles and lumps, and homogenous. The ability of the gel to spread out is essential for ensuring consistent application to the skin and patient compliance. A superior gel will be easy to spread and quick to spread. Gels containing 1% Carbopol 934 had a viscosity of  $74559 \pm 156$  CP, were very uniform, and spread out 4.6 times more readily than gels containing a lower concentration of

Carbopol 934. NBH NLC gel with a pH of 6.81 was effective, indicating it does not pose a significant risk of skin irritation when used transdermally.

### 3.9. *In vitro* release study.

NBH showed biphasic *in vitro* release from optimized NLC, with an initial burst release ( $12.3 \pm 0.31\%$  in 1 h) followed by a constant release, totaling  $96.76 \pm 0.28\%$  over the subsequent 12 h. The initial burst release of NBH from NLC could have been due to erosion of the superficial NBH in the NLC, or to the presence of most of the capryol 90 in the nanoparticles' outer region, forming a drug-enhanced shell that could cause burst release in the initial stage. NBH, a lipophilic drug, was quickly dissolved in the liquid lipid capryol 90, with more decadent outer layers due to their softness and improved solubility. Diffusion or erosion might then release a greater quantity of NBH. In contrast, the lipid encircled by the drug at the nanoparticle's center during manufacture would be responsible for the prolonged release profile (Figure 6).

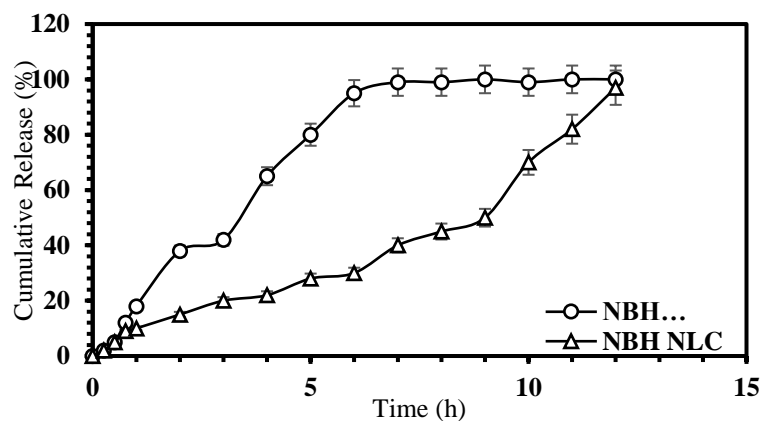


**Figure 6.** *In vitro* drug release from NBH NLC and NBH suspension.

### 3.10. *Ex vivo* skin permeation study.

After 24 h of *in vitro* skin permeation, the transdermal flux of NBH conventional gel was determined to be  $13.5 \pm 0.05$  g/cm<sup>2</sup>/h, whereas that of NBH NLC gel was  $45.7 \pm 0.8$  g/cm<sup>2</sup>/h. Maximum drug delivery was achieved with optimized NBH NLC gel compared to NBH conventional gel; the enhancement ratio was 3.20. The results showed that the permeability coefficient for NBH with the optimized NBH NLC was 0.045 cm/h, whereas that for NBH with the conventional NBH gel was 0.013 cm/h. The student's t-test demonstrated a statistically significant difference ( $p \leq 0.05$ ) in the means of transdermal flux. Due to the NLC's lipid film's occlusive qualities, skin moisture was increased, leading to greater drug penetration. Since the medication diffuses into deeper layers of skin through a concentration gradient in the solid phase, it is dermal. Effects are chemically stable and remain for a long time. The synergy between the lipid nanoparticle's occlusive action and the permeation-enhancing effects of the natural monoterpene (1,8-cineole) results in a significant increase in drug flow.

### 3.11. *In vivo* pharmacokinetic study.

The non-compartmental model was adopted for the pharmacokinetic evaluation. The pharmacokinetic parameters are provided in Table 6, and the plasma concentration-time profile

of NBH after oral administration and transdermal gel application in Wistar albino rats is illustrated in Figure 7.

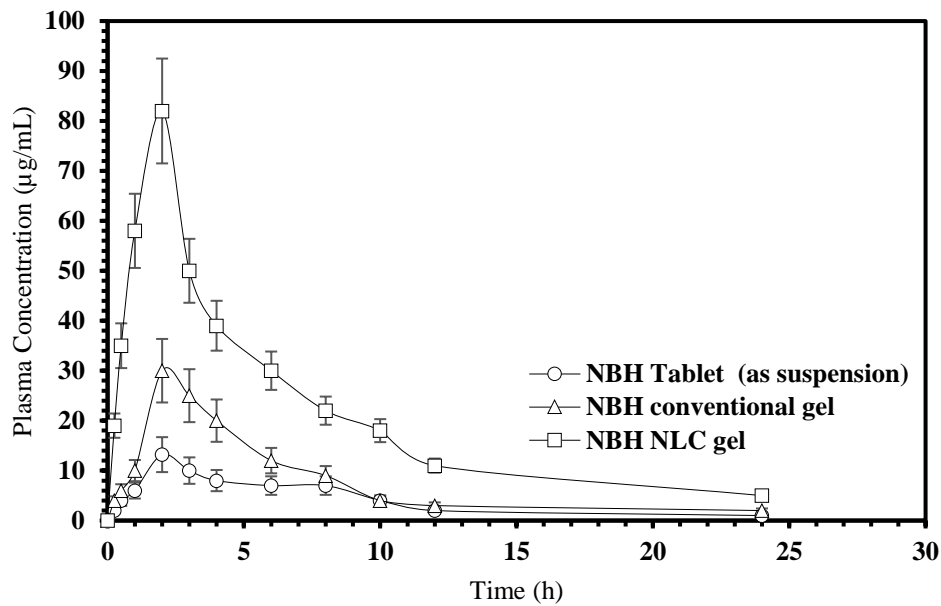


**Figure 7.** Plasma concentrations versus time profile of NBH following an oral suspension and transdermal NLC gel administration in Wistar albino rats.

T<sub>max</sub> values were 2.30± 0.20 h for the oral formulation, 2.15± 1.60 h for the conventional gel, and 1.98± 0.90 h for the NBH NLC gel. These values were more prominent than oral suspension (p≤ 0.001).

**Table 6.** Pharmacokinetic characteristics of oral, transdermal control, and transdermal NLC NBH in rats.

Pharmacokinetic parameters	NBH Tablet (as suspension)	NBH conventional gel	NBH NLC gel
<sup>a</sup> T <sub>max</sub> (h)	2.3± 0.20	2.15 ± 1.60	1.98 ± 0.89
<sup>b</sup> C <sub>max</sub> (ng/mL)	13.12	29.85	81.44
<sup>c</sup> AUC (ng.h/mL)	101.15	175.13	428.69
<sup>d</sup> t <sub>1/2</sub> (h)	6.34	11.51	12.29
K (h)	-0.109	-0.06	-0.03

<sup>a</sup> Time of peak concentration; <sup>b</sup> Peak of maximum plasma concentration; <sup>c</sup> Area under the concentration-time profile curve until last observation; <sup>d</sup> Half-life.

C<sub>max</sub> values for NBH NLC gel were reported to be 81.44 ng/mL, which was a significant improvement above C<sub>max</sub> values for the conventional gel (29.85 ng/mL) (p ≤ 0.001). The barrier properties of the stratum corneum explain why transdermal treatments exhibit lower C<sub>max</sub> and longer T<sub>max</sub>. The oral formulation, NBH conventional gel, showed AUCs of 101.15 ng.h/mL and 175.13 ng.h/mL, compared with 428.69 ng.h/mL for the NBH NLC gel. Compared with the conventional gel and oral formulation, the novel nano-lipid-based carrier shows a much higher AUC, suggesting superior absorption and better bioavailability. Perhaps the NBH NLC gel nanoparticles are responsible for its enhanced absorption. After the medication reaches the stratum corneum, an enormous increase in the interfacial area due to nanoparticles alters its transportability. The bioavailability of NBH from the NLC gel was threefold higher than that from the conventional gel and the oral formulation.

## 4. Conclusions

The NLC for the transdermal delivery of NBH was constructed and optimized using the Box-Behnken design. The suggested NLC formulation had a smaller particle size, a higher EE, and improved drug loading, and the experimentally measured results were quite close to design predictions. *In vitro* research employing NLC gel demonstrated greater drug penetration. Compared to the conventional gel of NBH with terpene, the addition of terpene to the NLC gel significantly increased the permeability of NBH through the skin of rats. The bioavailability of NBH was 3-fold higher *in vivo* due to improved skin permeability with the optimized formulation compared with the oral formulation. Our analysis revealed that the synthesized NLC could serve as a carrier for transdermal delivery of NBH. To thoroughly assess the potential of NLC loaded with NBH, further efficacy data is required.

## Author Contributions

Conceptualization, P.K. and S.P.; methodology, P.K.; S.R.; software, S.B.; validation, P.K., and S.R.; formal analysis, P.K.; investigation, P.K.; and S.P.; resources, P.K.; and S.P.; data curation, S.B.; writing—original draft preparation, S.P.; S.B.; writing—review and editing, S.P.; and S.B.; visualization, S.B.; supervision, S.P.; project administration, S.P.; funding acquisition, S.P. All authors have read and agreed to the published version of the manuscript.

## Institutional Review Board Statement

The animal study protocol was approved by the Institutional Review Board of the Department of Pharmaceutics, School of Pharmacy, Gurunanak Institutions Technical Campus (GNITC) (protocol code GNIP/CPCSEA/IAEC/2019/07 dated 03 Mar 2019).

## Informed Consent Statement

Not applicable.

## Data Availability Statement

Data supporting the findings of this study are available upon reasonable request from the corresponding author.

## Funding

This research received no external funding.

## Acknowledgments

The authors declare no acknowledgement.

## Conflicts of Interest

The authors declare no conflict of interest.

## References

1. Yurekli, A.A.; Bilir N.; Husain, M.J. Projecting burden of hypertension and its management in Turkey. *PLoS One* **2019**, *14*, e0221556, <https://doi.org/10.1371/journal.pone.0221556>.

2. Singh, B.; Khurana, L.; Bandyopadhyay, S.; Kapil, R.; Katare, O.O. Development of optimized self-nano-emulsifying drug delivery systems (SNEDDS) of carvedilol with enhanced bioavailability potential. *Drug Deliv.* **2011**, *18*, 599-612, <https://doi.org/10.3109/10717544.2011.604686>.
3. Mills, K.T.; Stefanescu, A.; He, J. The global epidemiology of hypertension. *Nat. Rev. Nephrol.* **2020**, *16*, 223-237, <https://doi.org/10.1038/s41581-019-0244-2>.
4. Shah, D.A.; Bhatt, K.K.; Mehta, R.S.; Baldania, S.L.; Gandhi, T.R. Stability Indicating RP-HPLC Estimation of Nebivolol Hydrochloride in Pharmaceutical Formulations. *Indian J. Pharm. Sci.* **2008**, *70*, 591-595, <https://doi.org/10.4103/0250-474X.45396>.
5. Ahad, A.; Al-Jenoobi, F.I.; Al-Mohizea, A.M.; Aqil, M.; Kohli, K. Transdermal delivery of calcium channel blockers for hypertension. *Expert Opin Drug Deliv* **2013**, *10*, 1137-1153, <https://doi.org/10.1517/17425247.2013.783562>.
6. Li, J.; Tian, S.; Tao, Q.; Zhao, Y.; Gui, R.; Yang, F.; Zang, L.; Chen, Y.; Ping, Q.; Hou, D. Montmorillonite/chitosan nanoparticles as a novel controlled-release topical ophthalmic delivery system for the treatment of glaucoma. *Int J Nanomed* **2018**, *13*, 3975-3987, <https://doi.org/10.2147/IJN.S162306>.
7. Amarachinta, P.R.; Sharma, G.; Samed, N.; Chettupalli, A.K.; Alle, M.; Kim, J.C. Central composite design for the development of carvedilol-loaded transdermal ethosomal hydrogel for extended and enhanced anti-hypertensive effect. *J Nanobiotechnol.* **2021**, *19*, 100, <https://doi.org/10.1186/s12951-021-00833-4>.
8. Pham, D.T.T.; Tran, P.H.L.; Tran, T.T.D. Development of solid dispersion lipid nanoparticles for improving skin delivery. *Saudi Pharm J* **2019**, *27*, 1019-1024, <https://doi.org/10.1016/j.jsps.2019.08.004>.
9. Ryakala, H.; Dineshmohan, S.; Ramesh, A.; Gupta, V.R. Formulation and in vitro evaluation of bilayer tablets of nebivolol hydrochloride and nateglinide for the treatment of diabetes and hypertension. *J Drug Deliv.* **2015**, *2015*, 827-859, <https://doi.org/10.1155/2015/827859>.
10. Uner, M.; Yener, G. Importance of solid lipid nanoparticles (SLN) in various administration routes and future perspectives. *Int J Nanomed* **2007**, *2*, 289-300.
11. Kim, K.H.; Jeon, Y.E.; Kang, S.; Lee, J.Y.; Lee, K.W.; Kim, K.T.; Kim, D.D. Lipid Nanoparticles for Enhancing the Physicochemical Stability and Topical Skin Delivery of Orobol. *Pharmaceutics* **2020**, *12*, 845, <https://doi.org/10.3390/pharmaceutics12090845>.
12. Jatav, V.S.; Saggi, J.S.; Sharma, A.K.; Sharma, A.; Jat, R.K. Design, development and permeation studies of nebivolol hydrochloride from novel matrix type transdermal patches. *Adv Biomed Res* **2013**, *2*, 62, <https://doi.org/10.4103/2277-9175.115813>.
13. Judd, E.; Calhoun, D.A. Apparent and true resistant hypertension: definition, prevalence and outcomes. *J Hum Hypertens* **2014**, *28*, 463-468, <https://doi.org/10.1038/jhh.2013.140>.
14. Hirlekar, R.; Patil, E.; Bhairy, S. Solid nanostructured lipid carriers loaded with silymarin for oral delivery: Formulation development and evaluation. *Curr Trends Pharm Pharm Chem* **2021**, *3*, 56-67, <https://doi.org/10.18231/j.ctppc.2021.014>.
15. Patel, S.; Shah, J.; Bhairy, S.; Hirlekar, R. Development of Curcumin loaded Nanostructured Lipid Carriers: Preparation, Characterization and In vitro Evaluation of Anti-cancer Activity Against A- 549 Human Lung Cancer Cell Line. *J. Cancer Tumor. Int.* **2021**, *11*, 66-88, <https://doi.org/10.9734/JCTI/2021/v11i430162>.
16. Bhairy, S.; Shaikh, A.; Nalawade, V.; Hirlekar, R. Development and validation of bivariate UV-visible spectroscopic method for simultaneous estimation of curcumin and piperine in their combined nanoparticulate system. *J. Appl. Pharm. Sci.* **2021**, *11*, 064-070, <https://doi.org/10.7324/JAPS.2021.110509>.
17. Alam, S.; Aslam, M.; Khan, A.; Imam, S.S.; Aqil, M.; Sultana, Y.; Ali, A. Nanostructured lipid carriers of pioglitazone for transdermal application: from experimental design to bioactivity detail. *Drug Deliv.* **2016**, *23*, 601-609, <https://doi.org/10.3109/10717544.2014.923958>.
18. Maulvi, F.A.; Thakkar, V.T.; Soni, T.G.; Gandhi, T.R. Optimization of aceclofenac solid dispersion using Box-Behnken design: *in vitro* and *in vivo* evaluation. *Curr. Drug Deliv.* **2014**, *11*, 380-391, <https://doi.org/10.2174/1567201811666140311103425>.
19. Shah, J.; Patel, S.; Bhairy, S.; Hirlekar, R. Formulation Optimization, Characterization and in Vitro Anti-Cancer Activity of Curcumin Loaded Nanostructured Lipid Carriers. *Int. J. Curr. Pharm. Res.* **2022**, *14*, 31-43, <https://doi.org/10.22159/ijcpr.2022v14i1.44110>.
20. Alshehri, S.; Imam, S.S. Formulation and evaluation of butenafine loaded PLGA-nanoparticulate laden chitosan nano gel. *Drug Deliv* **2021**, *28*, 2348-2360. <https://doi.org/10.1080/10717544.2021.1995078>.
21. Abdelwahed, W.; Degobert, G.; Stainmesse, S.; Fessi, H. Freeze-drying of nanoparticles: formulation, process and storage considerations. *Adv. Drug Deliv. Rev.* **2006**, *58*, 1688-1713, <https://doi.org/10.1016/j.addr.2006.09.017>.

22. Alam, P.; Siddiqui, N.A.; Rehman, M.T.; Hussain, A.; Akhtar, A.; Mir, S.R.; Alajmi, M.F. Box-Behnken Design (BBD)-Based Optimization of Microwave-Assisted Extraction of Parthenolide from the Stems of *Tarconanthus camphoratus* and Cytotoxic Analysis. *Molecules* **2021**, *26*, 1876, <https://doi.org/10.3390/molecules26071876>.
23. Ahad, A.; Aqil, M.; Kohli, K.; Sultana, Y.; Mujeeb, M.; Ali, A. Formulation and optimization of nanotransfersomes using experimental design technique for accentuated transdermal delivery of valsartan. *Nanomed.: Nanotechnol. Biol. Med.* **2012**, *8*, 237-249, <https://doi.org/10.1016/j.nano.2011.06.004>.
24. Pandey, S.S.; Maulvi, F.A.; Patel, P.S.; Shukla, M.R.; Shah, K.M.; Gupta, A.R.; Joshi, S.V.; Shah, D.O. Cyclosporine laden tailored microemulsion-gel depot for effective treatment of psoriasis: In vitro and in vivo studies. *Colloids Surf. B Biointerfaces* **2020**, *186*, 110681, <https://doi.org/10.1016/j.colsurfb.2019.110681>.
25. Intakhab, A.M.; Baboota, S.; Ahuja, A.; Ali, M.; Ali, J.; Kaur, S.J. Nanostructured Lipid Carrier Containing CNS Acting Drug: Formulation, Optimization and Evaluation. *Curr. Nanosci.* **2011**, *7*, 1014-1027, <https://doi.org/10.2174/1573413711107061014>.
26. Karishma, K.; Md, R.; Saima, A.; Showkat, R.M.; Sohail, A. Cilnidipine loaded transfersomes for transdermal application: Formulation optimization, *in vitro* and *in vivo* study. *J. Drug Deliv. Sci. Technol.* **2019**, *54*, 101303, <https://doi.org/10.1016/j.jddst.2019.101303>.
27. Ahad, A.; Aqil, M.; Kohli, K.; Sultana, Y.; Mujeeb, M. Design, formulation and optimization of valsartan transdermal gel containing iso-eucalyptol as novel permeation enhancer: preclinical assessment of pharmacokinetics in Wistar albino rats. *Expert Opin. Drug Deliv.* **2014**, *11*, 1149-1162, <https://doi.org/10.1517/17425247.2014.914027>.
28. Dai, Y.; But, P.P.; Chan, Y.P.; Matsuda, H.; Kubo, M. Antipruritic and antiinflammatory effects of aqueous extract from Si-Wu-Tang. *Biol. Pharm. Bull.* **2002**, *25*, 1175-1178, <https://doi.org/10.1248/bpb.25.1175>.
29. Ahad, A.; Aqil, M.; Ali, A. Investigation of anti-hypertensive activity of carbopol valsartan transdermal gel containing 1,8-cineole. *Int. J. Biol. Macromol.* **2014**, *64*, 144-149, <https://doi.org/10.1016/j.ijbiomac.2013.11.018>.
30. Han, F.; Yin, R.; Che, X.; Yuan, J.; Cui, Y.; Yin, H.; Li, S. Nanostructured lipid carriers (NLC) based topical gel of flurbiprofen: design, characterization and in vivo evaluation. *Int. J. Pharm.* **2012**, *439*, 349-357, <https://doi.org/10.1016/j.ijpharm.2012.08.040>.
31. Bhaskar, K.; Krishna, M.C.; Lingam, M.; Jagan, M.S.; Venkateswarlu, V.; Madhusudan, Y.R.; Bhaskar, K.; Anbu, J.; Ravichandran, V. Development of SLN and NLC enriched hydrogels for transdermal delivery of nitrendipine: in vitro and in vivo characteristics. *Drug Dev. Ind. Pharm.* **2009**, *35*, 98-113, <https://doi.org/10.1080/03639040802192822>.
32. Gedeon, C.; Kapur, B.; Aleksa, K.; Koren, G. A simple and rapid HPLC method for the detection of glyburide in plasma original research communication (analytical). *Clin. Biochem.* **2008**, *41*, 167-173, <https://doi.org/10.1016/j.clinbiochem.2007.07.025>.
33. Subedi, R.K.; Kang, K.W.; Choi, H.K. Preparation and characterization of solid lipid nanoparticles loaded with doxorubicin. *Eur. J. Pharm. Sci.* **2009**, *37*, 508-513, <https://doi.org/10.1016/j.ejps.2009.04.008>.
34. Alam, M.I.; Baboota, S.; Ahuja, A.; Ali, M.; Ali, J.; Sahni, S.K. Intranasal administration of nanostructured lipid carriers containing CNS acting drug: pharmacodynamic studies and estimation in blood and brain. *J. Psychiatr. Res.* **2012**, *46*, 1133-1138, <https://doi.org/10.1016/j.jpsychires.2012.05.014>.

## Publisher's Note & Disclaimer

The statements, opinions, and data presented in this publication are solely those of the individual author(s) and contributor(s) and do not necessarily reflect the views of the publisher and/or the editor(s). The publisher and/or the editor(s) disclaim any responsibility for the accuracy, completeness, or reliability of the content. Neither the publisher nor the editor(s) assume any legal liability for any errors, omissions, or consequences arising from the use of the information presented in this publication. Furthermore, the publisher and/or the editor(s) disclaim any liability for any injury, damage, or loss to persons or property that may result from the use of any ideas, methods, instructions, or products mentioned in the content. Readers are encouraged to independently verify any information before relying on it, and the publisher assumes no responsibility for any consequences arising from the use of materials contained in this publication.